Diversity of the isotope effect due to the energy-varying electronic density of states on strong-coupling superconductors

Yasushi Yokoya
Department of Applied Physics, Science University of Tokyo, 1-3 Kagurazaka, Shinjuku-ku, Tokyo 162, Japan
(Received 26 December 1996; revised manuscript received 6 May 1997)

We study superconducting critical temperatures within the strong-coupling Migdal-Eliashberg theory to clarify how the isotope effect is affected by the energy dependence of the electronic density of states (EDOS). In the computational procedure, we determine self-consistently both the electron self-energy in the normal state and the shift of the chemical potential. These quantities reflect asymmetry of energy dependence of the EDOS around the Fermi energy. As a result, we find that the energy dependence of the EDOS can reduce or enhance the isotope effect, and in some cases, it can make the isotope effect almost zero. [S0163-1829(97)08334-3]

I. INTRODUCTION

The strong-coupling Migdal-Eliashberg theory (M-E theory) has been a useful approach for the explanation of the superconducting properties in traditional phonon-mediated superconductors because of its theoretical reliability and practical usefulness.[1] However, it has been known also that it is not powerful enough in analyzing physical properties of recent unusual superconductors such as high-T_c cuprates and alkali-metal-doped fullerenes. These materials have unique physical properties, which cannot be explained by the conventional M-E theory. Among those physical properties, particularly, the isotope effect is one of the most interesting issues, because it is profoundly related to the mechanism of superconductivity. The isotope exponent, α, which is defined by

$$\alpha \equiv -\frac{d\ \ln T_c}{d\ \ln M}, \tag{1}$$

is equal to 0.5 in the usual weak-coupling BCS theory.[2] Here, T_c and M denote the superconducting critical temperature and the atomic mass, respectively. In general, $\alpha = 0.5$ does not hold exactly for real materials. One of the most typical points which is ignored in the weak-coupling BCS theory, is the Coulombic repulsion between electrons. It is well-known that α becomes smaller than 0.5 when the effects of this repulsion are added to the weak-coupling BCS theory[3] or the M-E theory.[4] The isotope effects found in the aforementioned materials are very anomalous, so that it seems to be very difficult to explain them within the conventional M-E theory. In high-T_c cuprates, α becomes almost zero,[5] negative,[6] or larger than 0.5.[7,8] On the other hand, in alkali-metal-doped fullerenes, α is rather large ($\alpha > 1$),[9,10] or is of normal value ($\alpha \leqslant 0.5$).[11,12] In addition to these anomalous values of α, the relation between α and T_c is also unusual for high-T_c cuprates; the magnitude of α decreases as T_c increases with the variation of the carrier concentration.[6–8] This relation between α and T_c also seems to be very difficult to explain by the M-E theory even though it takes account of the Coulombic repulsion between electrons, because α is an increasing function of T_c in the M-E theory.[4] Therefore, we study the origin of these anomalous isotope effects.

For this purpose, taking account of energy dependence of the electronic density of states (EDOS) is one of the improvements, and this improvement has been known to successfully explain the anomalous features of A15 compounds.[13–16] In high-T_c cuprates and alkali-metal-doped fullerenes, the EDOS's are supposed to vary rapidly near the Fermi energy. This is pointed out to be realistic by recent angle-resolved photoemission spectroscopy experiments[17–21] and recent band-structure calculations for high-T_c cuprate[22–25] and for alkali-metal-doped fullerenes.[26–28] Furthermore, both materials, high-T_c cuprates and alkali-metal-doped fullerenes, are known to have narrower electronic bands and wider phonon bands than the traditional superconductors have.[29–31] Therefore their EDOS's are expected to vary around the Fermi energy appreciably in the energy range whose width is comparative to the width of the phonon bands. Regarding these situations, the inclusion of energy dependence of the EDOS into the M-E theory is inevitably required to study the origin of the anomalous isotope effects of these materials.

The purpose of our study is to clarify how the isotope exponents, α, of strong-coupling superconductors are affected by taking account of energy dependence of the EDOS into the M-E theory. Standing on this point of view, there have been several works of high-T_c cuprates.[32–34] Our theoretical standing point in this paper is the M-E theory taking account of the energy dependence of the EDOS with an arbitrary value of a number of electrons. An important difference between our calculations and the series of works previously done by others is that our calculations assure the conservation of the number of electrons by the selfconsistent determination of the shift of the chemical potential. This requirement of the conservation of the number of electrons becomes important for an asymmetric shape of the EDOS around the Fermi energy, because the chemical potential shifts from a bare band one as a result of electron-phonon interactions. Although the resulting shift of the chemical potential is generally small, it is expected to affect α, because the isotope shifts of T_c are really small quantities. In this

work, we study how the isotope effects are affected by the shape of the EDOS, and examine how these effects depend on the coupling strength of electron-phonon interactions. Furthermore, the effect of a shape of the EDOS on α is examined in detail on the manner of the variation of the quasiparticle density of states (QDOS).

This paper is organized as follows. In Sec. II, the calculational method is given. In Sec. III, the numerical results are shown. Discussions on these results are given in Sec. IV.

II. CALCULATIONAL METHOD

A. Eliashberg equations

The superconducting critical temperature, T_c, in the isotropic M-E theory involving an energy-dependent EDOS can be obtained by solving the Eliashberg equations on the imaginary-frequency axis. The Eliashberg equations on the imaginary-frequency axis involving the Lorentzian type EDOS are originally developed by Mitrović and Carbotte,[16] and are written as

$$\widetilde{\Delta}_n=\frac{1}{\beta}\sum_{m=-\infty}^{\infty}\{\lambda(n-m)-\mu^*(\omega_c)\theta(\omega_c-|\omega_m|)\}\times\int_{-\infty}^{\infty}d\epsilon\,\frac{N(\epsilon)}{N(0)}\,\frac{\widetilde{\Delta}_m}{\widetilde{\omega}_m^2+(\epsilon-\delta\mu+\widetilde{\chi}_m)^2+\widetilde{\Delta}_m^2}, \quad (2a)$$

$$\widetilde{\omega}_n=\omega_n+\frac{1}{\beta}\sum_{m=-\infty}^{\infty}\lambda(n-m)\times\int_{-\infty}^{\infty}d\epsilon\,\frac{N(\epsilon)}{N(0)}\,\frac{\widetilde{\omega}_m}{\widetilde{\omega}_m^2+(\epsilon-\delta\mu+\widetilde{\chi}_m)^2+\widetilde{\Delta}_m^2}, \quad (2b)$$

$$\widetilde{\chi}_n=-\frac{1}{\beta}\sum_{m=-\infty}^{\infty}\lambda(n-m)\times\int_{-\infty}^{\infty}d\epsilon\,\frac{N(\epsilon)}{N(0)}\,\frac{\epsilon-\delta\mu+\widetilde{\chi}_m}{\widetilde{\omega}_m^2+(\epsilon-\delta\mu+\widetilde{\chi}_m)^2+\widetilde{\Delta}_m^2}, \quad (2c)$$

with

$$\lambda(n-m)=\int_0^{\infty}d\Omega\,\alpha^2F(\Omega)\,\frac{2\Omega}{\Omega^2+(\omega_n-\omega_m)^2}. \quad (2d)$$

We calculate T_c by solving these equations directly without a linealization of these equations; T_c is determined as the temperature, at which the anomalous electron self-energy, $\widetilde{\Delta}_n$, vanishes for every indices n of the Matsubara-frequency for the Fermions, $\omega_n=(2n+1)\pi/\beta$, where $\beta=1/k_BT$. Here, the function $\alpha^2F(\omega)$ is an electron-phonon spectral function, and μ^* is the Coulomb pseudopotential with a cutoff frequency ω_c. The anomalous (off-diagonal) electron self-energy, $\widetilde{\Delta}_n$, and the renormalized frequency, $\widetilde{\omega}_n$, are related to the gap function, $\Delta(i\omega_n)$, and the renormalization function, $Z(i\omega_n)$, by relations as $\widetilde{\Delta}_n\equiv\Delta(i\omega_n)Z(i\omega_n)$ and $\widetilde{\omega}_n\equiv\omega_nZ(i\omega_n)$. $\widetilde{\chi}_n$ is a diagonal part of the electron self-energy, and $\delta\mu$ expresses a shift of the chemical potential due to electron-phonon interactions. These two quantities, $\widetilde{\chi}_n$ and $\delta\mu$, have finite values for a general shape of the energy-dependent EDOS. In the calculation of T_c, not only the off-diagonal part of the electron self-energy but also the diagonal part depends explicitly on the atomic mass through the phonon Green's function which is included in $\alpha^2F(\omega)$. Therefore, $\widetilde{\chi}_n$ and $\delta\mu$ should not be ignored as long as isotope effects are considered.

B. Model of the electronic density of states

In the following numerical calculations, we use a Lorentzian type EDOS as a bare-band EDOS, which is given by

$$\frac{N(\epsilon)}{N(0)}=\frac{1}{1+x}\left(1+\frac{a^2x}{a^2+(\epsilon+b)^2}\right). \quad (3)$$

The EDOS, $N(\epsilon)$, is a single-spin EDOS, and the electronic energy, ϵ, is measured with respect to the bare-band structure chemical potential, b. The parameter, a, is a width of the bare-band Lorentzian type EDOS and x measures the prominence of energy variation of the EDOS. When x vanishes, Eq. (3) represents the Fermi-surface-restricted Eliashberg theory, which assumes a constant EDOS at the Fermi energy. To the contrary, when $x\to\infty$, Eq. (3) is reduced to the following form, which is written as

$$\frac{N(\epsilon)}{N(0)}=\frac{a^2}{a^2+(\epsilon+b)^2}. \quad (4)$$

In this case, we can determine the number of electrons as $n=(1/\pi)\tan^{-1}(b/a)+1/2$. The shift in the chemical potential, $\delta\mu$, is determined self-consistently by the supplementary equation which expresses the conservation of the number of electrons;

$$n=\frac{1}{2}-\frac{N(0)}{\beta}\sum_{m=0}^{\infty}\int_{-\infty}^{\infty}d\epsilon\,\frac{N(\epsilon)}{N(0)}\times\frac{\epsilon-\delta\mu+\widetilde{\chi}_m}{\widetilde{\omega}_m^2+(\epsilon-\delta\mu+\widetilde{\chi}_m)^2+\widetilde{\Delta}_m^2}. \quad (5)$$

By solving these Eq. (2) and Eq. (5), we obtain temperature-dependent quantities, $\widetilde{\Delta}_n$, $\widetilde{\omega}_n$, $\widetilde{\chi}_n$, and $\delta\mu$, for a given number of electrons, n. (This notation n should not be confused with the index, n, of the Matsubara frequency appearing as the suffix in the imaginary-axis quantities, such as $\widetilde{\Delta}_n$, $\widetilde{\omega}_n$, and $\widetilde{\chi}_n$.)

Throughout this paper, we show only the results with a restricted value of the parameter, $a=2\Omega_{\max}$, in the EDOS, $N(\epsilon)$.

C. Model of the electron-phonon spectral function

Following the calculational procedure, we can carry out our numerical work once the electron-phonon spectral function, $\alpha^2F(\omega)$, is determined. In the following numerical analysis, we employ the Lorentzian type model function of $\alpha^2F(\omega)$, which is given by

$$\alpha^2F(\omega) = \begin{cases} \dfrac{d^2}{d^2+(2\omega-\Omega_{\max})^2} - \dfrac{d^2}{d^2+\Omega_{\max}^2}, & 0 \leqslant \omega \leqslant \Omega_{\max}, \\ 0, & \Omega_{\max} < \omega. \end{cases} \tag{6}$$

Here, $\Omega_{\max}$ is the maximum phonon frequency. We choose the parameters, $d=5$ meV and $\Omega_{\max}=80$ meV, respectively. In order to calculate the isotope exponent, α, we introduce the dimensionless parameter, η, which is given by

$$\eta = \frac{M}{M_0}. \tag{7}$$

Here, M_0 and M mean an initial atomic mass and a substituent isotope mass, respectively. Since any $\alpha^2F(\omega)$ depends on the atomic mass as a square root,[4] the width of the model function of $\alpha^2F(\omega)$ for a substituent isotope becomes $\omega_{\max}/\sqrt{\eta}$. In other words, d and $\Omega_{\max}$ in Eq. (6) are replaced with $d/\sqrt{\eta}$ and $\Omega_{\max}/\sqrt{\eta}$, respectively, by the isotope substitution. In the following calculations of the isotope exponent, α, we use the value of atomic mass ratio, $\eta=1.125$, in the case of the high-T_c cuprates (^{18}O substitution for ^{16}O).

III. NUMERICAL RESULTS

In this section, the electron self-energy in the normal state, $\tilde{\chi}_n$, and the shift of the chemical potential, $\delta\mu$, are calculated. We calculate these quantities to examine how the asymmetry of shape of the EDOS around the Fermi energy affects isotope effects.

A. Effect of the normal state electron self-energy

In this subsection, we present only the results for $\mu^*=0.175$. Before examining isotope effects, we study the influence of the electron self-energy in the normal state, $\tilde{\chi}_n$, on the superconducting critical temperatures, T_c. In the calculation of T_c, we use the Lorentzian type EDOS given in Eq. (3). In Fig. 1, curves of T_c versus the scaled bare-band chemical potential, $b/\Omega_{\max}$, are shown for $x=3$ (solid line), 6 (dashed-dotted line), 15 (dashed line), 50 (broken line) and $x\to\infty$(dotted line), respectively. These curves are calculated by (a) taking account of $\tilde{\chi}_n$ and (b) neglecting $\tilde{\chi}_n$, respectively. The value of $\tilde{\chi}_n$ vanishes when $b=0$, because the EDOS is symmetrical around the Fermi energy. Therefore, the curves of (a) and (b) connect with each other at the center of the figure ($b=0$). The difference between (a) and (b) becomes noticeable as x increases, where the curves of (a) drop more rapidly than that of (b) as b increases. As a result, we can see that the effect of $\tilde{\chi}_n$ becomes important as x increases.

Now let us examine a role of $\tilde{\chi}_n$ in isotope effects. Isotope effects are calculated for the Lorentzian type EDOS given in Eq. (3). In Fig. 2, curves of the isotope exponent, α, versus $b/\Omega_{\max}$, are shown for $x=3$ (solid line), 6 (dashed-dotted line), 15 (dashed line), 50 (broken line) and $x\to\infty$ (dotted line), respectively. These curves are calculated by (a) taking account of $\tilde{\chi}_n$ and (b) neglecting $\tilde{\chi}_n$, respectively. $\tilde{\chi}_n$ vanishes when $b=0$ by the same reason of the calculation of T_c. Therefore, the curves of (a) and (b) also connect with each other at the center of the figure ($b=0$). In Fig. 2, it is noted that the curves of α decrease as x increases in Fig. 2(a), while the curves of α increase in Fig. 2(b). This means that the effect of $\tilde{\chi}_n$ becomes important as the energy dependence of the EDOS becomes sharp. In Fig. 2(b), there is a peak structure in the curve of α at $b/\Omega_{\max}\sim3$, and it becomes higher and higher as x increases. In Fig. 2(a), on the other hand, there is only a little peak structure for small x, and it vanishes as x increases. By looking at a position of the peak structure, we can find that the degree of influence of $\tilde{\chi}_n$ is proportional to the degree of slope of the

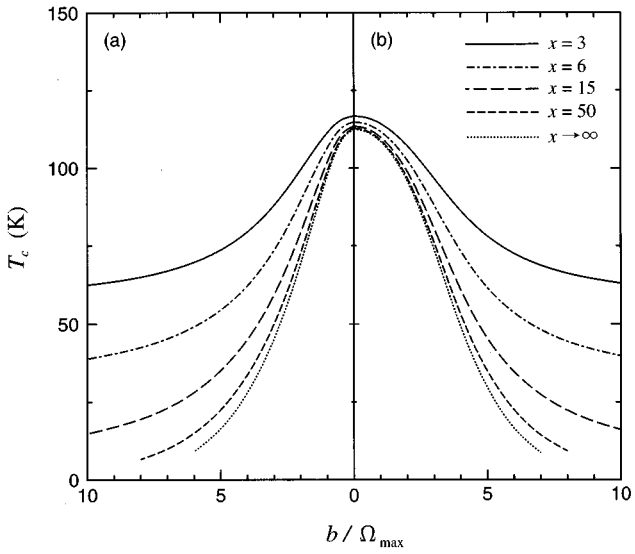

FIG. 1. Curves of T_c versus $b/\Omega_{\max}$ for $x=3$ (solid line), 6 (dashed-dotted line), 15 (dashed line), 50 (broken line), and $x\to\infty$ (dotted line), respectively. The curves are calculated by (a) taking account of $\tilde{\chi}_n$ and (b) neglecting $\tilde{\chi}_n$, respectively.

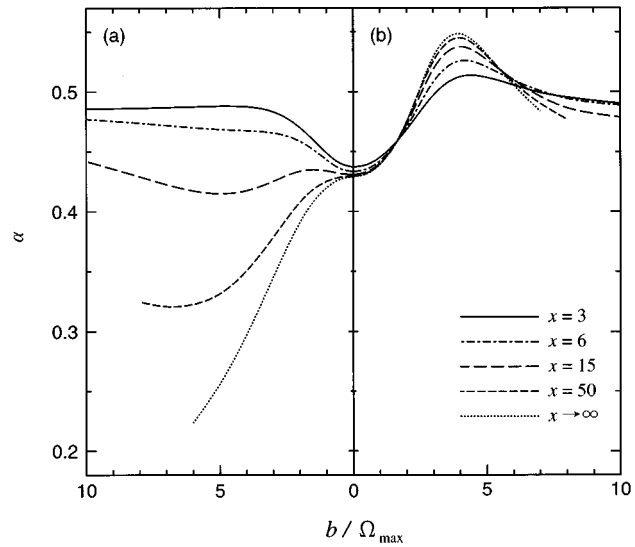

FIG. 2. Curves of the isotope exponent, α, versus $b/\Omega_{\max}$ for $x=3$ (solid line), 6 (dashed-dotted line), 15 (dashed line), 50 (broken line) and $x\to\infty$ (dotted line), respectively. The curves are calculated by (a) taking account of $\tilde{\chi}_n$ and (b) neglecting $\tilde{\chi}_n$, respectively.

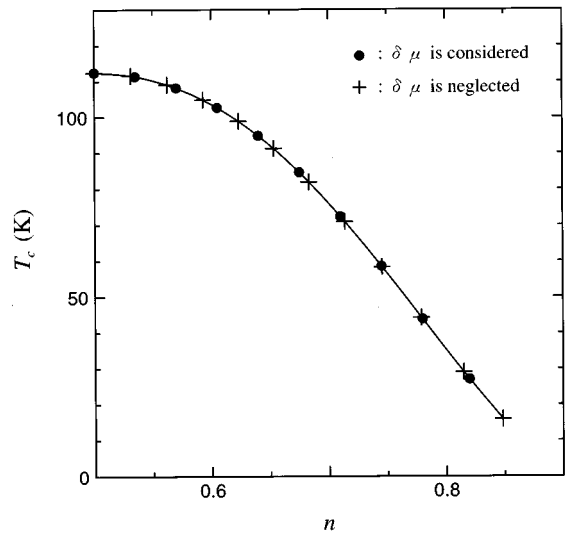

FIG. 3. Curves of T_c as a function of number of electrons, n. The curves are calculated by taking account of the shift of the chemical potential, $\delta\mu$, (solid circle), and neglecting $\delta\mu$ (plus), respectively.

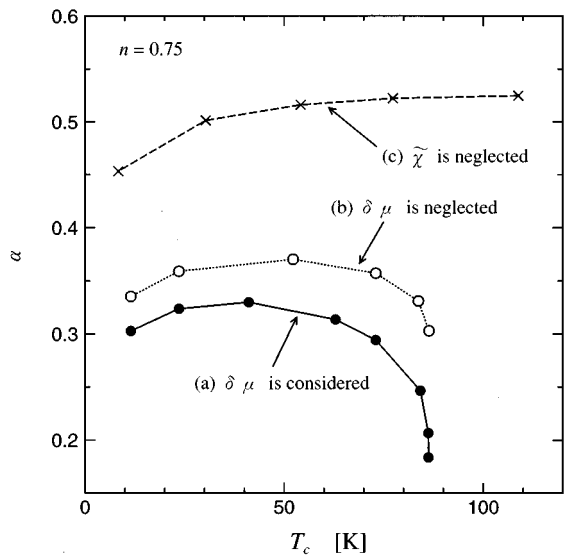

FIG. 4. Curves of the isotope exponent, α, versus T_c are shown for $n=0.75$: (a) solid circles are calculated by taking account of both $\tilde{\chi}_n$ and $\delta\mu$; (b) open circles are calculated by taking account of only $\tilde{\chi}_n$; (c) crosses are calculated in disregard of both $\tilde{\chi}_n$ and $\delta\mu$.

EDOS at the Fermi energy, because the derivative of the EDOS with respect to ϵ is large in this region. Moreover, in Fig. 2, curves of α seem to approach the particular value, $\alpha\sim 0.47$, as b increases, where the EDOS becomes flat. In fact, the value of $\alpha=0.472$ is given by the Eliashberg theory with the Fermi-surface-restricted approximation, where the effect of the energy dependence of the EDOS vanishes exactly by the assumption of a constant density of states at the Fermi energy.

B. Effect of the shift of the chemical potential

We have described the effects of the electron self-energy in the normal state, $\tilde{\chi}_n$, to the isotope exponent, α. Now let us see the role of the shift of the chemical potential, $\delta\mu$, on the isotope effect. Although the magnitude of $\delta\mu$ is small, we should examine the effects of $\delta\mu$ on α, because α is very sensitive to the change of T_c.

Figure 3 shows curves of T_c as a function of a number of electrons, n. In the calculation of T_c, we use the Lorentzian type EDOS, Eq. (4). In this case, $\delta\mu$ can be determined self-consistently by Eq. (5). In Fig. 3, curves are calculated by taking account of $\delta\mu$ (solid circle) and neglecting $\delta\mu$ (plus), respectively. When $\delta\mu$ is considered, the chemical potential shifts as the result of electron-phonon interaction to conserve a number of electrons (solid circle). When $\delta\mu$ is neglected, on the other hand, the chemical potential is invariable and then a number of electrons change (plus) as a result. Therefore, the resulting value of n is different from each other. From Fig. 3, however, we can find that the effect of $\delta\mu$ on the value of T_c is negligibly small.

In Fig. 4, curves of α versus T_c are drawn for the fixed number of electrons, $n=0.75$. In this calculation, we calculate α by changing electron-phonon coupling strength. The curves of α are shown as follows: (a) solid circles are calculated by taking account of both $\tilde{\chi}_n$ and $\delta\mu$; (b) open circles are calculated by taking account of only $\tilde{\chi}_n$; (c) crosses are calculated by neglecting both $\tilde{\chi}_n$ and $\delta\mu$. In the numerical calculations of (b) and (c), therefore, the resulting number of electrons, $n=0.75$, is obtained by appropriate choice of the chemical potential. In Fig. 4, the curve of α considering both $\tilde{\chi}_n$ and $\delta\mu$ (a) is the lowest of all curves, while the curve neglecting both $\tilde{\chi}_n$ and $\delta\mu$ (c) is the highest. Therefore, we can find that the effect of $\delta\mu$ also reduces the isotope shift of T_c as well as $\tilde{\chi}_n$.

In Fig. 5, curves of α versus T_c are shown for $n=0.50$, 0.70, 0.75, and 0.80 (solid lines and circles) with the curve according to the Fermi-surface-restricted Eliashberg theory (dotted line and open circles), respectively. Figures 5(a) and 5(b) correspond to the results for the Coulomb pseudopotential $\mu^*=0$ and 0.175, respectively. The numerical results are given by taking account of both $\tilde{\chi}_n$ and $\delta\mu$, except the one according to the Fermi-surface-restricted Eliashberg theory (dotted lines and open circles), in which $\tilde{\chi}_n$ and $\delta\mu$ vanish exactly. In Fig. 5(b), the drop of α in the low-T_c (weak electron-phonon coupling) region is due to μ^* in the similar way as in the Fermi-surface-restricted Eliashberg theory.[4] In the high-T_c region, the curves of α (solid lines) which are calculated by taking account of both $\tilde{\chi}_n$ and $\delta\mu$, are decreasing functions whereas the curve of the Fermi-surface-restricted Eliashberg theory (dotted line) is an increasing function.[4] Furthermore, magnitude of α decreases as n increases. Particularly, at the large n ($n=0.75$ and 0.80), the magnitude of α decreases and can even vanish in the strong electron-phonon coupling (high-T_c) region.

To sum up the results obtained in this section, the value of α is reduced and, sometimes, can be almost zero by the effects of both the electron self-energy in the normal state, $\tilde{\chi}_n$, and the shift of the chemical potential, $\delta\mu$, which reflect the asymmetry of energy dependence of the EDOS around the Fermi energy. As a result, we can get various degrees of reduction of isotope effects by the Eliashberg equations with energy dependence of the EDOS.

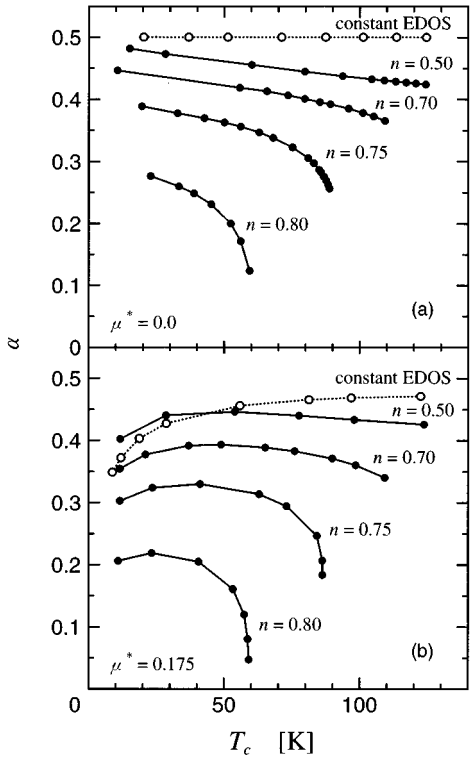

FIG. 5. Curves of the isotope exponent, α, versus T_c for $n=0.50$, 0.70, 0.75, and 0.80 (solid circle) with a curve according to the Fermi-surface-restricted Eliashberg theory (open circle), respectively. (a) and (b) correspond to the results for the Coulomb pseudopotential $\mu^*=0$ and 0.175, respectively. All these curves are calculated by taking account of both $\tilde{\chi}_n$ and $\delta\mu$, except the one by the Fermi-surface-restricted Eliashberg theory (open circles).

IV. DISCUSSION

First, we show the quasiparticle density of states (QDOS) to discuss the behavior of isotope exponents, α, of our results microscopically. The expression of the QDOS normalized by the bare-band EDOS at the Fermi energy $N(0)$, is given by the formula

$$\tilde{N}(\omega)=-\frac{1}{\pi}\,\mathrm{Im}\left[\int_{-\infty}^{\infty}d\epsilon\,\frac{N(\epsilon)}{N(0)}\times\frac{\tilde{\omega}(\omega)+\epsilon+\delta\mu-\tilde{\chi}(\omega)}{\tilde{\omega}^2(\omega)-[\epsilon-\delta\mu+\tilde{\chi}(\omega)]^2-\tilde{\Delta}^2(\omega)}\right]. \quad (8)$$

In this equation, $\tilde{\Delta}(\omega)$, $\tilde{\omega}(\omega)$, and $\tilde{\chi}(\omega)$ are real-axis quantities which are an analytic continuation of imaginary-axis quantities $\tilde{\Delta}_n$, $\tilde{\omega}_n$, and $\tilde{\chi}_n$, respectively. To calculate these real-axis quantities at an arbitrary temperature, we employ the MSC equations[35,36] as an analytic continuation method.

Figure 6 shows curves of the QDOS, $\tilde{N}(\omega)$, for (a) $T_c=49.45$ K (solid line), (b) 73.01 K (broken line), and (c) 84.23 K (dotted line), respectively. Here, all the curves are calculated at $T=T_c$ and total number of electrons, n, is fixed to 0.75. It can be seen from Fig. 6 that the damping effect due to the phonon scattering broadens the shape of $\tilde{N}(\omega)$ as a whole, as electron-phonon coupling strength increases. On the other hand, $\tilde{N}(\omega)$ has an additional sharp peak structure appearing around the Fermi energy, which originates from the mass enhancement effect due to the electron-phonon interaction. In the inset of Fig. 6, curves of $\tilde{N}(\omega)$ close up around the Fermi energy are shown. The value of T_c is strongly affected by the number of quasiparticles in the energy region whose width is about $\Omega_{\max}$ around the Fermi energy ($\epsilon\leqslant|\Omega_{\max}|$).[15,36] Therefore, the isotope effect can be expressed as the decreasing number of quasiparticles due to

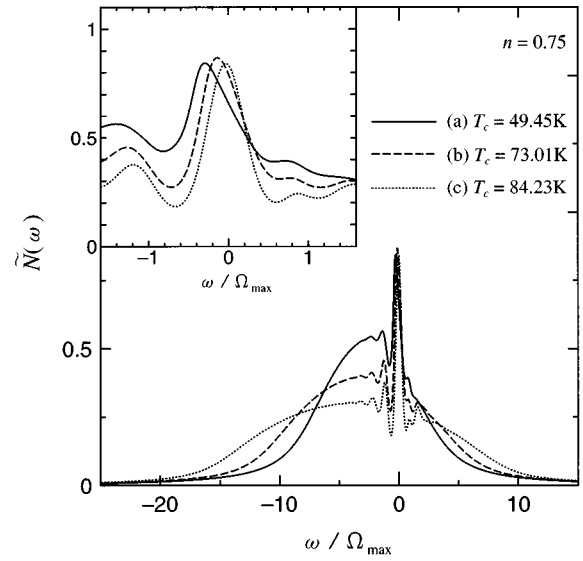

FIG. 6. Curves of the quasiparticle density of states (QDOS) in the normal state, $\tilde{N}(\omega)$, of $n=0.75$ are shown in cases of (a) $T_c=49.45$ K (solid line), (b) 73.01 K (broken line), and (c) 84.23 K (dotted line), respectively. All the curves are calculated at $T=T_c$. In the inset, curves of $\tilde{N}(\omega)$ close up around the Fermi energy are shown.

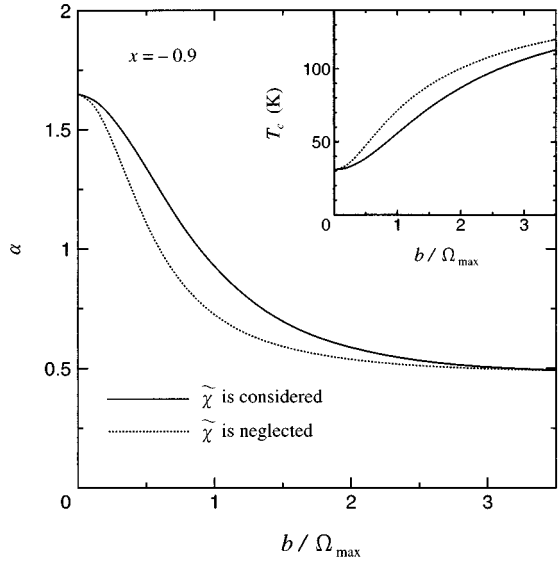

FIG. 7. Curves of isotope exponent, α, versus $b/\Omega_{\max}$ for $x=-0.9$ and $\mu^*=0$. The solid line is calculated by taking account of $\tilde{\chi}_n$ and dotted line is the one ignoring $\tilde{\chi}_n$, respectively. In the inset, curves of T_c versus $b/\Omega_{\max}$ are shown in the same parameter.

the narrowing of the energy region ($\Omega_{\max} \rightarrow \Omega_{\max}/\sqrt{\eta}$) under the isotope substitution. Roughly speaking, the value of α is in proportion to the ratio of this decreasing number of quasiparticles to the one in the energy region, $\epsilon \leqslant |\Omega_{\max}|$. From Fig. 6, it can be seen that this decreasing ratio of the number of quasiparticles for the lower T_c is larger than that for the higher T_c. As a result, α decreases as electron-phonon coupling strength increases.

Before closing this section, we mention the behavior of α for $x<0$, in Eq. (3), where the EDOS contains a hollow structure at the Fermi energy. For the isotope substitution, if $x<0$, the number of electrons relating with phonons decreases much more than that of the Fermi-surface-restricted Eliashberg theory. Therefore, the value of α is expected to be larger than 0.5. In Fig. 7, curves of α versus $b/\Omega_{\max}$ are shown for $x=-0.9$ and the Coulomb pseudopotential, $\mu^*=0$. In the inset, the curves of T_c versus $b/\Omega_{\max}$ are shown in the same parameter. In Fig. 7, solid lines are calculated by taking account of $\tilde{\chi}_n$, and dotted lines are the one neglecting $\tilde{\chi}_n$, respectively. In these figures, there is a distinct difference between the two lines (solid and dotted lines) as the result of the effect of $\tilde{\chi}_n$. The magnitude of α approaches 0.5 from 1.65 asymptotically as $b/\Omega_{\max}$ increases, where the EDOS becomes flat around the Fermi energy and then the contribution of $\tilde{\chi}_n$ decreases. This result is consistent with the large isotope effect of alkali-metal-doped fullerenes.[9,10] In fact, there are band-structure calculations of these materials, where the EDOS is expected to have a hollow structure around the Fermi energy.[26–28]

In this paper, we have studied the effects of energy variation of the EDOS on isotope effects by the M-E theory. The wide variety of the isotope exponent, α, is shown by the self-consistent calculation of the electron self-energy in the normal state, $\tilde{\chi}_n$, and the shift of the chemical potential, $\delta\mu$, at the fixed number of electrons. The point of our numerical results is that both $\tilde{\chi}_n$ and $\delta\mu$ affects the value of α strongly, whereas there is scarcely any effect of them to the value of T_c. These results are qualitatively different from the results by both the weak-coupling BCS theory and the Fermi-surface-restricted Eliashberg theory.

ACKNOWLEDGMENTS

The author would like to thank Y. Oi Nakamura and N. Tsuda for helpful discussions and encouragement. The author appreciates very constructive comments by Y. Shiina and Y. Suwa. Part of the numerical calculations were performed on FACOM VPP500 at the Supercomputer Center of Institute of Solid State Physics of University of Tokyo.

[1] D. J. Scalapino, in *Superconductivity Vol. 1*, edited by R. D. Parks (Marcel Dekker, New York, 1969), p. 449.

[2] J. Bardeen, L. N. Cooper, and J. R. Schrieffer, Phys. Rev. **108**, 1175 (1957).

[3] P. Morel and P. W. Anderson, Phys. Rev. **125**, 1263 (1962).

[4] J. P. Carbotte, Rev. Mod. Phys. **62**, 1027 (1990).

[5] B. Batlogg, R. J. Cava, A. Jayaraman, R. B. van Dover, G. A. Kourouklis, S. Sunshine, D. W. Murphy, L. W. Rupp, H. S. Chen, A. White, K. T. Short, A. M. Mujsce, and E. A. Rietman, Phys. Rev. Lett. **58**, 2333 (1987); B. Batlogg, G. Kourouklis, W. Weber, R. J. Cava, A. Jayaraman, A. E. White, K. T. Short, L. W. Rupp, E. A. Rietman, *ibid.* **59**, 912 (1987).

[6] H. J. Bornemann, D. E. Morris, and H. B. Liu, Physica C **182**, 132 (1991).

[7] M. K. Crawford, M. N. Kunchur, W. E. Farneth, E. M. McCarron III, and S. J. Poon, Phys. Rev. B **41**, 282 (1990).

[8] J. P. Franck, J. Jung, M. A.-K. Mohamed, S. Gygax, and G. I. Sproule, Phys. Rev. B **44**, 5318 (1991).

[9] T. W. Ebbesen, J. S. Tsai, K. Tanigaki, J. Tabuchi, Y. Shimakawa, Y. Kubo, I. Hirosawa, and J. Mizuki, Nature (London) **355**, 620 (1992).

[10] A. A. Zakhidov, K. Imaeda, D. M. Petty, K. Yakushi, H. Inokuchi, K. Kikuchi, I. Ikemoto, S. Suzuki, and Y. Achiba, Phys. Lett. A **164**, 355 (1992).

[11] A. P. Ramirez, A. R. Kortan, M. J. Rosseinsky, S. J. Duclos, A. M. Mujsce, R. C. Haddon, D. W. Murphy, A. V. Makhija, S. M. Zahurak, and K. B. Lyons, Phys. Rev. Lett. **68**, 1058 (1992).

[12] V. H. Crespi and M. L. Cohen, Phys. Rev. B **52**, 3619 (1995); B. Burk, V. H. Crespi, A. Zettl, and M. L. Cohen, Phys. Rev. Lett. **72**, 3706 (1994).

[13] P. B. Allen and B. Mitrović, in *Solid State Physics*, edited by H. Ehrenreich, F. Seitz, and D. Turnbull (Academic, New York, 1982), Vol. 37, pp. 1–92.

[14] W. E. Pickett, Phys. Rev. B **21**, 3897 (1980); **26**, 1186 (1982); W. E. Pickett and B. M. Klein, Solid State Commun. **38**, 95 (1981).

[15] S. G. Lie and J. P. Carbotte, Solid State Commun. **35**, 127 (1980); **34**, 599 (1980); **26**, 511 (1978).

[16] B. Mitrović and J. P. Carbotte, Can. J. Phys. **61**, 784 (1983); **61**, 758 (1983).

[17] Jian Ma, C. Quitmann, R. J. Kelley, P. Almé ras, H. Berger, G. Margaritondo, and M. Onellion, Phys. Rev. B **51**, 3832 (1995).

[18] A. A. Abrikosov, J. C. Campuzano, and K. Gofron, Physica C **214**, 73 (1993); K. Gofron, J. C. Campuzano, H. Ding, C. Gu, R. Liu, B. Dabrowski, B. W. Veal, W. Cramer, and G. Jennings, J. Phys. Chem. Solids **54**, 1193 (1993).

[19] J. C. Campuzano, G. Jennings, M. Faiz, L. Beaulaigue, B. W. Veal, J. Z. Liu, A. P. Paulikas, K. Vandervoort, H. Claus, R. S. List, A. J. Arko, and R. J. Bartlett, Phys. Rev. Lett. **64**, 2308 (1990).

[20] C. G. Olson, R. Liu, D. W. Lynch, R. S. List, A. J. Arko, B. W. Veal, Y. C. Chang, P. Z. Jiang, and A. P. Paulikas, Phys. Rev. B **42**, 381 (1990).

[21] D. S. Dessau, Z.-X. Shen, D. M. King, D. S. Marshall, L. W. Lombardo, P. H. Dickinson, A. G. Loeser, J. DiCarlo, C.-H. Park, A. Kapitulnik, and W. E. Spicer, Phys. Rev. Lett. **71**, 2781 (1993); Z.-X. Shen, C. K. Shih, O. Jepsen, W. E. Spicer, I. Lindau, and J. W. Allen, *ibid.* **64**, 2442 (1990).

[22] J. Yu, S. Massidda, A. J. Freeman, and D. D. Koelling, Phys. Lett. A **122**, 203 (1987); S. Massidda, J. Yu, A. J. Freeman, and D. D. Koelling, *ibid.* **122**, 198 (1987).

[23] W. E. Pickett, Rev. Mod. Phys. **61**, 433 (1989).

[24] H. Krakauer, W. E. Pickett, and R. E. Cohen, Phys. Rev. B **47**, 1002 (1993).

[25] O. K. Andersen, O. Jepsen, A. I. Liechtenstein, and I. I. Mazin, Phys. Rev. B **49**, 4145 (1994).
[26] S. C. Erwin and W. E. Pickett, Science **254**, 842 (1991).
[27] M.-Z. Huang, Y.-N. Xu, and W. Y. Ching, Phys. Rev. B **47**, 8249 (1994); **46**, 6572 (1992); J. Chem. Phys. **96**, 1648 (1992).
[28] S. Satpathy, V. P. Antropov, O. K. Andersen, O. Jepsen, O. Gunnarsson, and A. I. Liechtenstein, Phys. Rev. B **46**, 1773 (1992).
[29] B. Renker, F. Gompf, D. Ewert, P. Adelmann, H. Schmidt, E. Gering, and H. Mutka, Z. Phys. B **77**, 65 (1989); B. Renker, F. Gompf, E. Gering, N. Nücker, D. Ewert, W. Reichardt, and H. Rietschel, *ibid.* **67**, 15 (1987).
[30] S. Mase and T. Yasuda, J. Phys. Soc. Jpn. **58**, 658 (1989).
[31] K. Prassides, J. Tomkinson, C. Christides, M. J. Rosseinsky, D. W. Murphy, and R. C. Haddon, Nature (London) **354**, 462 (1991).
[32] E. Schachinger, M. G. Greeson, and J. P. Carbotte, Phys. Rev. B **42**, 406 (1990); J. P. Carbotte and R. Akis, Solid State Commun. **82**, 613 (1992); P. J. Williams and J. P. Carbotte, Phys. Rev. B **45**, 7984 (1992).
[33] R. J. Radtke and M. R. Norman, Phys. Rev. B **50**, 9554 (1994).
[34] A. A. Abrikosov, J. Phys. Chem. Solids **56**, 1567 (1995); Physica C **233**, 102 (1994).
[35] F. Marsiglio, M. Schossmann, and J. P. Carbotte, Phys. Rev. B **37**, 4965 (1988).
[36] Y. Yokoya and Y. Oi Nakamura, Solid State Commun. **98**, 133 (1996); Physica C **262**, 187 (1996).